Available online at www.sciencedirect.com
ScienceDirect
Journal of Sound and Vibration 300 (2007) 993–1014
JOURNAL OF SOUND AND VIBRATION
www.elsevier.com/locate/jsvi

Resonances and resonant frequencies for a class of nonlinear systems

Z.K. Peng*, Z.Q. Lang, S.A. Billings

Department of Automatic Control and Systems Engineering, University of Sheffield, Mappin Street, Sheffield S1 3JD, UK

Received 3 April 2006; received in revised form 27 July 2006; accepted 12 September 2006
Available online 2 November 2006

Abstract

Resonant phenomena for a class of nonlinear systems, which can be described by a single-degree-of-freedom (sdof) model with a polynomial-type nonlinear stiffness, are investigated using nonlinear output frequency response functions (NOFRFs). The concepts of resonance and resonant frequencies are proposed for this class of nonlinear systems using the NOFRF concept, and the effects of damping on the resonances and resonant frequencies are analyzed. These results produce a novel interpretation of energy transfer phenomena in this class of nonlinear systems and show how the damping effect influences the system resonant frequencies and amplitudes. The results are important for the design and fault diagnosis of mechanical systems and structures which can be described by the sdof nonlinear model.

1. Introduction

Resonance is a well-known concept in linear system analysis. At a resonance, the frequency of an exciting force matches the natural frequency of the system so that the energy transmission is efficient, and the amplitude of vibration can become significant. The study of resonances is important in many branches of engineering. For example, in mechanical and civil engineering design, vehicle design [1], the design of steam-turbine rotor-bearing systems [2], and bridge design [3], and the design of vibration controllers and isolators [4,5]. Understanding resonances is important to ensure an appropriate running condition and a desired behavior of the systems. Most studies of resonance assume the system is linear. However, in engineering many dynamical systems have nonlinear components, which cannot simply be described by a linear model. For example, vibration components with clearances [6,7] and motion limiting stops [8,9] or vibration components with fatigue damage [10,11], which cause abrupt changes in the stiffness and damping coefficients, represent a significant proportion of these systems. To investigate such nonlinear systems, nonlinear oscillators have been widely adopted. For example, the bilinear oscillator, piecewise linear oscillator and cubic stiffness oscillator [12] are often used to describe the changes of stiffness with operating conditions. In engineering practice and laboratory research activities, resonance phenomena have also been observed in nonlinear systems. It has been observed that, when the excitation frequency is half the eigenfrequency of a cracked object, vibrations often

*Corresponding author.
E-mail addresses: z.peng@sheffield.ac.uk (Z.K. Peng), z.lang@sheffield.ac.uk (Z.Q. Lang).

0022-460X/$ - see front matter © 2006 Elsevier Ltd. All rights reserved.
doi:10.1016/j.jsv.2006.09.012

become significant. The resonance at the eigenfrequency is a similar effect to the resonance of a linear system, but the resonance at half the eigenfrequency is a phenomenon unique to nonlinear systems, and is known as the secondary resonance [13–15]. In addition, a one-third eigenfrequency resonance has also been observed in a system with a nonlinear stiffness [16]. Although the importance of the resonance for linear systems is well known and the phenomena of resonances have been observed in nonlinear systems, surprisingly, there are no equivalent concepts about resonances and resonant frequencies for nonlinear systems.

Unlike linear systems where the dynamic properties can be simply described by the system frequency response function (FRF), the description of the dynamic properties of nonlinear systems is much more complicated. A comprehensive investigation of the issue of resonances and resonant frequencies for nonlinear systems is complicated because there are no tools which are capable of tackling problems for all nonlinear systems. The Volterra series approach [17–19] is a powerful tool for the analysis of nonlinear systems, which extends the familiar concept of the convolution integral for linear systems to a series of multidimensional convolution integrals. The Fourier transforms of the Volterra kernels, called generalized frequency response functions (GFRFs) [20], are an extension of the linear FRF to the nonlinear case. If a differential equation or discrete-time model is available for a nonlinear system, the GFRFs can be determined using the algorithm in Refs. [21–23]. However, the GFRFs are multidimensional functions [24,25], which are much more complicated than the linear FRF and are often difficult to measure, display and interpret in practice. Recently, a novel concept known as nonlinear output frequency response functions (NOFRFs) was proposed by the authors [26]. The concept can be considered to be an alternative extension of the classical FRF for linear systems to the nonlinear case. NOFRFs are one-dimensional functions of frequency, which allow the analysis of nonlinear systems to be implemented in a manner similar to the analysis of linear systems and which provide great insight into the mechanisms which dominate many nonlinear behaviors.

In the present study, based on the concept of NOFRFs, the phenomenon of resonance is studied for a class of nonlinear systems which can be described by a single-degree-of-freedom (sdof) model with a polynomial-type nonlinear stiffness. The effects of damping on the resonances and resonant frequencies are analyzed. The results are useful for the study of energy transfer phenomena for this class of nonlinear systems and for investigating the effects of damping on the nonlinear behavior. These results are important for the design and fault diagnosis of mechanical systems and structures which can be described by an sdof nonlinear model.

2. sdof nonlinear systems with polynomial-type stiffness

In engineering, there are many dynamical systems with nonlinear components, most of which can be described as an sdof systems with different nonlinear spring characteristics as shown in Eq. (1) [12]:

$$m\ddot{x}(t) + c\dot{x}(t) + s(x(t)) = f_0(t). \tag{1}$$

In Eq. (1), m and c, are the object mass and damping coefficient, respectively; $x(t)$ is the displacement, and $s(x)$ is the restoring force which is a nonlinear function of $x(t)$. Some of the most commonly used nonlinear restoring force representations can be found in Ref. [12]. Fig. 1 gives some of these results, which have been widely used in mechanical and structural behavior studies. For example, a crack in a beam can be modelled as a bilinear stiffness oscillator [10,11], the connection between a control surface and servoactuator in an aircraft wing [27] can be expressed as a spring with piecewise linear stiffness, and a planetary gear system [28] with multiple clearances can be described as a clearance-type nonlinear system shown in Fig. 1(c).

In mathematics, the Weierstrass approximation theorem [29] guarantees that any continuous function on a closed and bounded interval can be uniformly approximated on that interval by a polynomial to any degree of accuracy. All the nonlinear restoring forces in Fig. 1 are continuous functions of displacement x; and can therefore be approximated by a polynomial. Fig. 2 shows a polynomial approximation for a piecewise linear stiffness restoring force.

With a polynomial approximation of the restoring force $s(x)$, the sdof nonlinear system (1) can be described by a polynomial-type nonlinear system, as

$$m\ddot{x} + c\dot{x} + \sum_{i=1}^{n} k_i x^i = f_0(t), \tag{2}$$

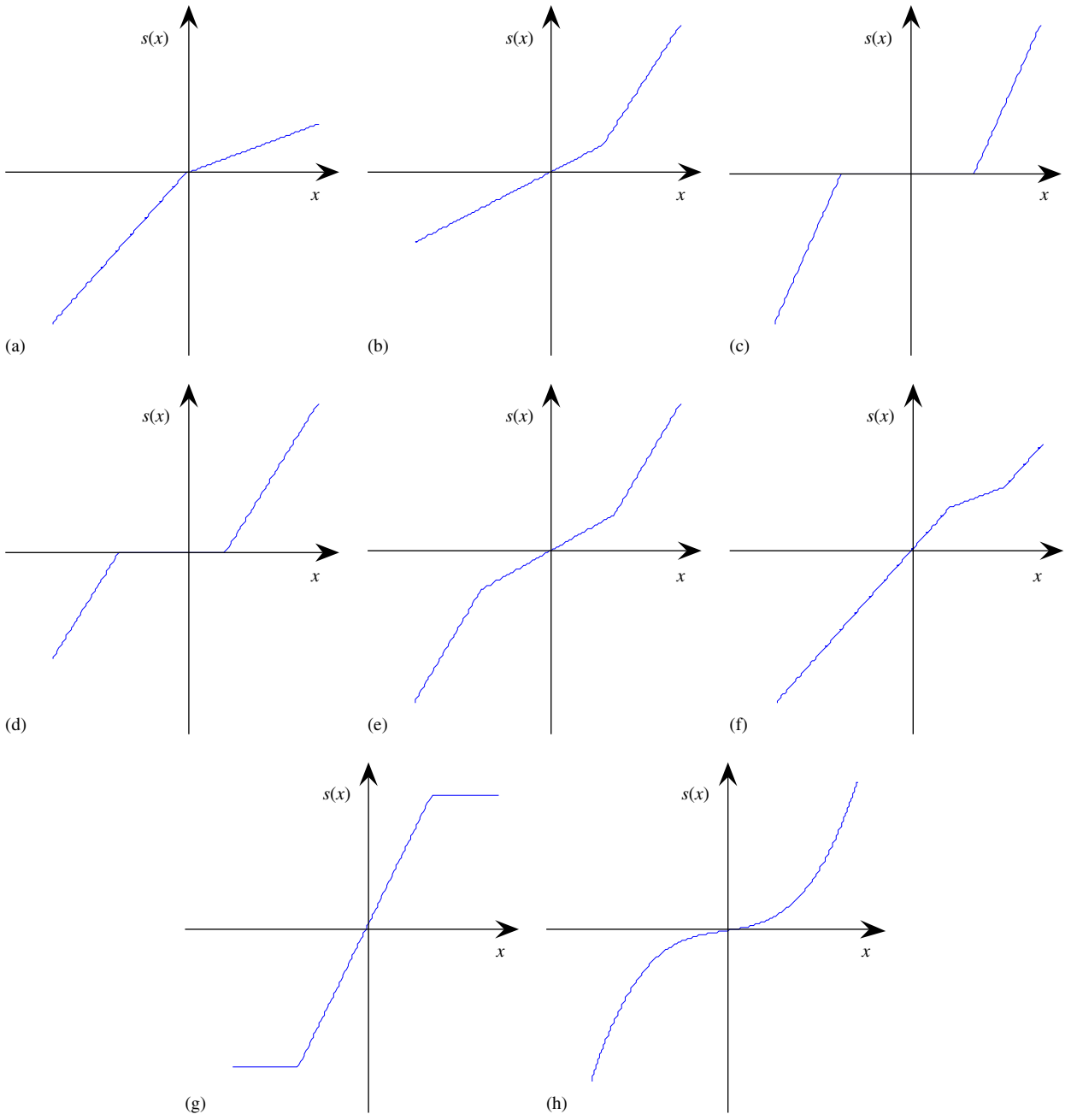

Fig. 1. Most commonly used representations of nonlinear restoring force: (a) bilinear stiffness, (b) bilinear stiffness with offset, (c) clearance, (d) off-center clearance, (e) piecewise linear stiffness, (f) pre-loaded piecewise linear stiffness, (g) saturation, and (h) cubic stiffness.

where n is the order of the approximating polynomial, and k_i, $(i = 1, \ldots, n)$ are the characteristic parameters of the restoring force $s(x)$.

Because many nonlinear systems and structures can be approximated by polynomial-type nonlinear systems, an investigation of the polynomial-type nonlinear systems will be important for understanding and explaining complicated nonlinear phenomena caused by linear components in mechanical systems and structures. The Volterra series theory of nonlinear systems is the basis of the study of a wide class of nonlinear systems including the polynomial-type nonlinear system given by Eq. (2). The concepts of GFRFs [20,30,31]

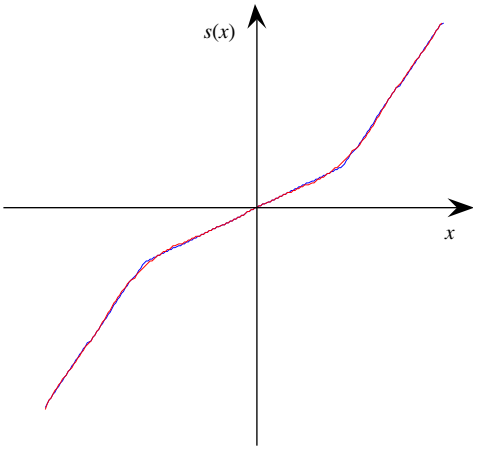

Fig. 2. A polynomial approximation of a piecewise linear restoring force.

and NOFRFs are the frequency domain representations of the nonlinear systems which can be described by a Volterra series model.

GFRFs and NOFRFs are the extensions of the FRF of linear systems to the nonlinear case from two different perspectives. However, the NOFRFs are a one-dimensional function of frequency. This allows the analysis of nonlinear systems in the frequency domain to be implemented in a manner similar to the analysis of linear system FRFs, and consequently provides a convenient way to analyze resonance phenomena of a class of nonlinear systems.

3. Nonlinear output frequency response functions (NOFRFs)

3.1. NOFRFs under general inputs

NOFRFs were recently proposed and used to investigate the behavior of structures with polynomial-type nonlinearities [26]. The definition of NOFRFs is based on the Volterra series theory of nonlinear systems. The Volterra series extends the familiar concept of the convolution integral for linear systems to a series of multidimensional convolution integrals.

Consider the class of nonlinear systems which are stable at zero equilibrium and which can be described in the neighborhood of the equilibrium by the Volterra series

$$y(t)=\sum_{n=1}^{N}\int_{-\infty}^{\infty}\cdots\int_{-\infty}^{\infty}h_n(\tau_1,\ldots,\tau_n)\prod_{i=1}^{n}u(t-\tau_i)\,\mathrm{d}\tau_i, \tag{3}$$

where $y(t)$ and $u(t)$ are the output and input of the system, $h_n(\tau_1,...,\tau_n)$ is the nth-order Volterra kernel, and N denotes the maximum order of the system nonlinearity. Lang and Billings [20] have derived an expression for the output frequency response of this class of nonlinear systems to a general input. The result is

$$\begin{cases} Y(j\omega)=\sum_{n=1}^{N}Y_n(j\omega) \quad \text{for } \forall\omega, \\ Y_n(j\omega)=\dfrac{1/\sqrt{n}}{(2\pi)^{n-1}} \quad \int_{\omega_1+,\ldots,+\omega_n=\omega}H_n(j\omega_1,\ldots,j\omega_n)\prod_{i=1}^{n}U(j\omega_i)\,\mathrm{d}\sigma_{n\omega}. \end{cases} \tag{4}$$

This expression reveals how nonlinear mechanisms operate on the input spectra to produce the system output frequency response. In Eq. (4), $Y(j\omega)$ is the spectrum of the system output, $Y_n(j\omega)$ represents the

nth-order output frequency response of the system

$$H_n(j\omega_1,\ldots,j\omega_n)=\int_{-\infty}^{\infty}\cdots\int_{-\infty}^{\infty}h_n(\tau_1,\ldots,\tau_n)e^{-(\omega_1\tau_1+,\ldots,+\omega_n\tau_n)j}\,d\tau_1,\ldots,d\tau_n \tag{5}$$

is the definition of the GFRF, and

$$\int_{\omega_1+,\ldots,+\omega_n=\omega}H_n(j\omega_1,\ldots,j\omega_n)\prod_{i=1}^{n}U(j\omega_i)\,d\sigma_{n\omega}$$

denotes the integration of $H_n(j\omega_1,...,j\omega_n)\prod_{i=1}^{n}U(j\omega_i)$ over the n-dimensional hyper-plane $\omega_1+\cdots+\omega_n=\omega$. Eq. (4) is a natural extension of the well-known linear relationship $Y(j\omega)=H_1(j\omega)U(j\omega)$ to the nonlinear case.

For linear systems, the possible output frequencies are the same as the frequencies in the input. For nonlinear systems described by Eq. (3), however, the relationship between the input and output frequencies is more complicated. Fortunately, given the frequency range of the input, the output frequencies of system (3) can be determined using an explicit expression derived by Lang and Billings in Ref. [20].

Based on the above results for output frequency responses of nonlinear systems, a new concept known as the NOFRF was recently introduced by Lang and Billings [26]. The concept was defined as

$$G_n(j\omega)=\frac{\int_{\omega_1+,\ldots,+\omega_n=\omega}H_n(j\omega_1,...,j\omega_n)\prod_{i=1}^{n}U(j\omega_i)\,d\sigma_{n\omega}}{\int_{\omega_1+,\ldots,+\omega_n=\omega}\prod_{i=1}^{n}U(j\omega_i)\,d\sigma_{n\omega}} \tag{6}$$

under the condition that

$$U_n(j\omega)=\int_{\omega_1+,\ldots,+\omega_n=\omega}\prod_{i=1}^{n}U(j\omega_i)\,d\sigma_{n\omega}\neq 0. \tag{7}$$

Note that $G_n(j\omega)$ is valid over the frequency range of $U_n(j\omega)$, which can be determined using the algorithm in Ref. [20].

By introducing the NOFRFs $G_n(j\omega)$, $n=1,\ldots N$, Eq. (4) can be written as

$$Y(j\omega)=\sum_{n=1}^{N}Y_n(j\omega)=\sum_{n=1}^{N}G_n(j\omega)U_n(j\omega), \tag{8}$$

which is similar to the description of the output frequency response of linear systems. For a linear system, the relationship between $Y(j\omega)$ and $U(j\omega)$ can be illustrated as in Fig. 3. Similarly, the nonlinear system input and output relationship of Eq. (3) can be illustrated in Fig. 4.

The NOFRFs reflect a combined contribution of the system and the input to the frequency domain output behavior. It can be seen from Eq. (6) that $G_n(j\omega)$ depends not only on H_n $(n=1,\ldots,N)$ but also on the input $U(j\omega)$. For any structure, the dynamical properties are determined by the GFRFs H_n $(n=1,\ldots,N)$. However, from Eq. (5) it can be seen that the GFRF is multidimensional [24,25], which makes it difficult to measure, display and interpret the GFRFs in practice. Feijoo et al. [32–34] demonstrated that the Volterra series can be described by a series of associated linear equations (ALEs) whose corresponding associated frequency response functions (AFRFs) are easier to analyze and interpret than the GFRFs. According to Eq. (6), the NOFRF $G_n(j\omega)$ is a weighted sum of $H_n(j\omega_1,\ldots,j\omega_n)$ over $\omega_1+\cdots+\omega_n=\omega$ with the weights depending on the test input. Therefore, $G_n(j\omega)$ can be used as alternative representation of the structural dynamical properties described by H_n. The most important property of the NOFRF $G_n(j\omega)$ is that it is one dimensional, and thus allows the analysis of nonlinear systems to be implemented in a convenient manner similar to the analysis of linear systems. Moreover, there is an effective algorithm [26] available which allows the estimation

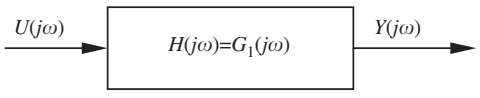

Fig. 3. The output frequency response of a linear system.

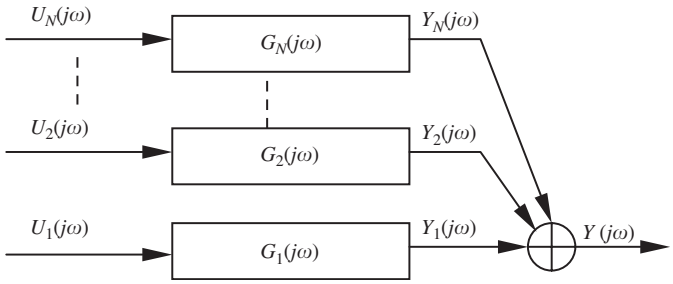

Fig. 4. The output frequency response of a nonlinear system.

of the NOFRFs to be implemented directly using system input output data. This algorithm is briefly introduced in below.

Rewrite Eq. (8) as

$$[Y(j\omega)] = [U_1(j\omega), \ldots, U_N(j\omega)][G(j\omega)], \tag{9}$$

where $[G(j\omega)] = [G_1(j\omega), \ldots, G_N(j\omega)]^{\mathrm{T}}$.

Consider the case of $u(t) = \alpha u^*(t)$ where α is a constant and $u^*(t)$ is the input signal under which the NOFRFs of the system are to be evaluated, then

$$\begin{aligned} U_n(j\omega) &= \frac{1/\sqrt{n}}{(2\pi)^{n-1}} \int_{\omega_1+,\ldots,+\omega_n=\omega} \prod_{i=1}^{n} U(j\omega_i)\, \mathrm{d}\sigma_{n\omega} \\ &= \alpha^n \frac{1/\sqrt{n}}{(2\pi)^{n-1}} \int_{\omega_1+,\ldots,+\omega_n=\omega} \prod_{i=1}^{n} U^*(j\omega_i)\, \mathrm{d}\sigma_{n\omega} = \alpha^n U_n^*(j\omega), \end{aligned} \tag{10}$$

where $U^*(j\omega)$ is the Fourier transform of $u^*(t)$ and

$$U_n^*(j\omega) = \frac{1/\sqrt{n}}{(2\pi)^{n-1}} \int_{\omega_1+,\ldots,+\omega_n=\omega} \prod_{i=1}^{n} U^*(j\omega_i)\, \mathrm{d}\sigma_{n\omega}.$$

In this case, it is known from Eq. (9) that

$$[Y(j\omega)] = [\alpha U_1^*(j\omega), \ldots, \alpha^N U_N^*(j\omega)][G^*(j\omega)], \tag{11}$$

where $[G^*(j\omega)] = [G_1^*(j\omega), \ldots, G_N^*(j\omega)]^{\mathrm{T}}$ which are the NOFRFs to evaluate.

Excite the system under study $\bar{N}$ times by the input signals $\alpha_i u^*(t)$, $i = 1, \ldots, \bar{N}$, where $\bar{N} \geqslant N$ and $\alpha_{\bar{N}}, \alpha_{\bar{N}-1}, \ldots, \alpha_1$ are constants which satisfy the condition

$$\alpha_{\bar{N}} > \alpha_{\bar{N}-1} > \cdots > \alpha_1 > 0.$$

$\bar{N}$ output frequency responses $Y^i(j\omega)$, $i = 1, \ldots, \bar{N}$ can be generated for a system under study. From Eq. (11), it is known that the output frequency responses can be related to the NOFRFs to be evaluated as below:

$$\mathbf{Y}^{1,\ldots,\bar{N}}(j\omega) = \mathbf{A}\mathbf{U}^{1,\ldots,\bar{N}}(j\omega)[G^*(j\omega)], \tag{12}$$

where

$$\mathbf{Y}^{1,\ldots,\bar{N}}(j\omega) = [Y^1(j\omega), \ldots, Y^{\bar{N}}(j\omega)]^{\mathrm{T}} \tag{13}$$

and

$$\mathbf{A}\mathbf{U}^{1,\ldots,\bar{N}}(j\omega) = \begin{bmatrix} \alpha_1 U_1^*(j\omega), \ldots, \alpha_1^N U_N^*(j\omega) \\ \vdots \\ \alpha_{\bar{N}} U_1^*(j\omega), \ldots, \alpha_{\bar{N}}^N U_N^*(j\omega) \end{bmatrix}. \tag{14}$$

Consequently, the values of the NOFRFs, $G_1^*(j\omega),\ldots,G_N^*(j\omega)$, can be determined using a least-squares-based approach as

$$[G^*(j\omega)]=[G_1^*(j\omega),\ldots,G_N^*(j\omega)]^{\mathrm{T}}=[(\mathbf{AU}^{1,\ldots,\tilde{N}}(j\omega))^{\mathrm{T}}(\mathbf{AU}^{1,\ldots,\tilde{N}}(j\omega))]^{-1}(\mathbf{AU}^{1,\ldots,\tilde{N}}(j\omega))^{\mathrm{T}}\mathbf{Y}^{1,\ldots,\tilde{N}}(j\omega). \tag{15}$$

3.2. NOFRFs under harmonic input

Harmonic inputs are pure sinusoidal signals which have been widely used for dynamic testing of many engineering structures. Therefore, the extension of the NOFRF concept to the harmonic input case is of considerable engineering significance.

When system (3) is subject to a harmonic input

$$u(t)=A\cos(\omega_F t+\beta). \tag{16}$$

Lang and Billings [20] showed that Eq. (3) can be expressed as

$$Y(j\omega)=\sum_{n=1}^{N}Y_n(j\omega)=\sum_{n=1}^{N}\left(\frac{1}{2^n}\sum_{\omega_{k_1}+\cdots+\omega_{kn}=\omega}H_n(j\omega_{k_1},\ldots,j\omega_{k_n})A(j\omega_{k_1})\cdots A(j\omega_{k_n})\right), \tag{17}$$

where

$$A(j\omega)=\begin{cases}|A|\mathrm{e}^{j\mathrm{sign}(k)\beta} & \text{if } \omega\in\{k\omega_F,k=\pm1\},\\ 0 & \text{otherwise.}\end{cases} \tag{18}$$

Define the frequency components of nth-order output of the system as Ω_n, according to Eq. (17), the frequency components in the system output can be expressed as

$$\Omega_n=\bigcup_{n=1}^{N}\Omega_n \tag{19}$$

and Ω_n is determined by the set of frequencies

$$\{\omega=\omega_{k_1}+\cdots+\omega_{k_n}|\omega_{k_i}=\pm\omega_F,\ i=1,\ldots,n\}. \tag{20}$$

From Eq. (20), it is known that if all $\omega_{k_1},\ldots,\omega_{k_n}$ are taken as $-\omega_F$, then $\omega=-n\omega_F$. If k of them are taken as ω_F, then $\omega=(-n+2k)\omega_F$. The maximal k is n. Therefore, the possible frequency components of $Y_n(j\omega)$ are

$$\Omega_n=\{(-n+2k)\omega_F,\ \ k=0,1,\ldots,n\}. \tag{21}$$

Moreover, it is easy to deduce that

$$\Omega=\bigcup_{n=1}^{N}\Omega_n=\{k\omega_F,k=-N,\ldots,-1,0,1,\ldots,N\}. \tag{22}$$

Eq. (22) explains why some superharmonic components will be generated when a nonlinear system is subjected to a harmonic excitation. In the following, only those components with positive frequencies will be considered.

The NOFRFs defined in Eq. (6) can be extended to the case of harmonic inputs as

$$G_n^H(j\omega)=\frac{\frac{1}{2^n}\sum_{\omega_{k_1}+\cdots+\omega_{kn}=\omega}H_n(j\omega_{k_1},\ldots,j\omega_{k_n})A(j\omega_{k_1})\ldots A(j\omega_{k_n})}{\frac{1}{2^n}\sum_{\omega_{k_1}+\cdots+\omega_{kn}=\omega}A(j\omega_{k_1})\ldots A(j\omega_{k_n})}\quad n=1,\ldots,N \tag{23}$$

under the condition that

$$A_n(j\omega)=\frac{1}{2^n}\sum_{\omega_{k_1}+\cdots+\omega_{kn}=\omega}A(j\omega_{k_1})\ldots A(j\omega_{k_n})\neq0. \tag{24}$$

Obviously, $G_n^H(j\omega)$ is only valid over Ω_n defined by Eq. (21). Consequently, the output spectrum $Y(j\omega)$ of nonlinear systems under a harmonic input can be expressed as

$$Y(j\omega) = \sum_{n=1}^{N} Y_n(j\omega) = \sum_{n=1}^{N} G_n^H(j\omega) A_n(j\omega). \tag{25}$$

when k of the n frequencies of $\omega_{k_1}, \ldots, \omega_{k_n}$ are taken as ω_F and the others are as $-\omega_F$, substituting Eq. (18) into Eq. (24) yields

$$A_n(j(-n+2k)\omega_F) = \frac{1}{2^n} C_n^k |A|^n \, \mathrm{e}^{j(-n+2k)\beta}. \tag{26}$$

Thus $G_n^H(j\omega)$ becomes

$$\begin{aligned} G_n^H(j(-n+2k)\omega_F) &= \frac{\frac{1}{2^n} H_n(\overbrace{j\omega_F, \ldots, j\omega_F}^{k}, \overbrace{-j\omega_F, \ldots, -j\omega_F}^{n-k}) C_n^k |A|^n \, \mathrm{e}^{j(-n+2k)\beta}}{\frac{1}{2^n} C_n^k |A|^n \, \mathrm{e}^{j(-n+2k)\beta}} \\ &= H_n(\overbrace{j\omega_F, \ldots, j\omega_F}^{k}, \overbrace{-j\omega_F, \ldots, -j\omega_F}^{n-k}) \end{aligned} \tag{27}$$

where $H_n(j\omega_1, \ldots, j\omega_n)$ is assumed to be a symmetric function. Therefore, in this case, $G_n^H(j\omega)$ over the nth-order output frequency range $\Omega_n = \{(-n+2k)\omega_F, k = 0, 1, \ldots, n\}$ is equal to the GFRF $H_n(j\omega_1, \ldots, j\omega_n)$ evaluated at $\omega_1 = \cdots = \omega_k = \omega_F, \omega_{k+1} = \cdots = \omega_n = -\omega_F$, $k = 0, \ldots, n$.

3.3. NOFRFs of the polynomial-type nonlinear systems under harmonic inputs

By setting

$$\varsigma = \frac{c}{2\sqrt{k_1/m}}, \quad \omega_L = \sqrt{\frac{k_1}{m}}, \quad \varepsilon_i = \frac{k_i}{k_1} \ \ (i = 2, \ldots, n), \quad f_0(t) = \frac{f(t)}{m}$$

the polynomial-type nonlinear system (2) can be expressed in a standard form

$$\ddot{x} + 2\varsigma\omega_L \dot{x} + \omega_L^2 x + \sum_{i=2}^{n} \varepsilon_2 \omega_L^2 x^n = f_0(t). \tag{28}$$

The first nonlinear output FRF can easily be determined from the linear part of Eq. (28) as

$$G_1^H(j\omega) = H_1(j\omega) = \frac{1}{(j\omega)^2 + 2\varsigma\omega_L(j\omega) + \omega_L^2}. \tag{29}$$

The GFRF up to 4th order can be calculated recursively using the algorithm by Billings and Peyton Jones [22,23] to produce the results below:

$$H_2(j\omega_1, j\omega_2) = -\varepsilon_2 \omega_L^2 H_1(j\omega_1) H_1(j\omega_2) H_1(j\omega_1 + j\omega_2), \tag{30}$$

$$\begin{aligned} H_3(j\omega_1, j\omega_2, j\omega_3) = & -\omega_L^2 \Big\{ \frac{2}{3} \varepsilon_2 [H_1(j\omega_1) H_2(j\omega_2, j\omega_3) + H_1(j\omega_2) H_2(j\omega_1, j\omega_3) + H_1(j\omega_3) H_2(j\omega_1, j\omega_2)] \\ & + \varepsilon_3 H_1(j\omega_1) H_1(j\omega_2) H_1(j\omega_3) \Big\} H_1(j\omega_1 + j\omega_2 + j\omega_3), \end{aligned} \tag{31}$$

$$\begin{aligned} H_4(j\omega_1, j\omega_2, j\omega_3, j\omega_4) = & -\omega_L^2 H_1(j\omega_1 + j\omega_2 + j\omega_3 + j\omega_4) [\varepsilon_2 H_{42}(j\omega_1, j\omega_2, j\omega_3, j\omega_4) \\ & + \varepsilon_3 H_{43}(j\omega_1, j\omega_2, j\omega_3, j\omega_4) + \varepsilon_4 H_{44}(j\omega_1, j\omega_2, j\omega_3, j\omega_4)], \end{aligned} \tag{32}$$

where

$$H_{42}(j\omega_1,j\omega_2,j\omega_3,j\omega_4) = \frac{1}{2}[H_1(j\omega_1)H_3(j\omega_2,j\omega_3,j\omega_4) + H_1(j\omega_2)H_3(j\omega_1,j\omega_3,j\omega_4) + H_1(j\omega_3)H_3(j\omega_1,j\omega_2,j\omega_4) + H_1(j\omega_4)H_3(j\omega_1,j\omega_2,j\omega_3)] + \frac{1}{3}[H_2(j\omega_1,j\omega_2)H_2(j\omega_3,j\omega_4) + H_2(j\omega_1,j\omega_3)H_2(j\omega_2,j\omega_4) + H_2(j\omega_1,j\omega_4)H_2(j\omega_2,j\omega_3)], \tag{33}$$

$$H_{43}(j\omega_1,j\omega_2,j\omega_3,j\omega_4) = \frac{1}{2}[H_1(j\omega_1)H_1(j\omega_2)H_2(j\omega_3,j\omega_4) + H_1(j\omega_1)H_1(j\omega_3)H_2(j\omega_2,j\omega_4) + H_1(j\omega_1)H_1(j\omega_4)H_2(j\omega_2,j\omega_3) + H_1(j\omega_2)H_1(j\omega_3)H_2(j\omega_1,j\omega_4) + H_1(j\omega_2)H_1(j\omega_4)H_2(j\omega_1,j\omega_3) + H_1(j\omega_3)H_1(j\omega_4)H_2(j\omega_1,j\omega_2)], \tag{34}$$

$$H_{44}(j\omega_1,j\omega_2,j\omega_3,j\omega_4) = H_1(j\omega_1)H_1(j\omega_2)H_1(j\omega_3)H_1(j\omega_4). \tag{35}$$

From Eqs. (30) to (35), it can be observed that $H_4(j\omega_1,j\omega_2,j\omega_3,j\omega_4)$, $H_3(j\omega_1,j\omega_2,j\omega_3)$ and $H_2(j\omega_1,j\omega_2)$ are symmetric functions. Therefore, when system (28) is subjected to a harmonic loading, the NOFRFs of the system can be described as

$$G_2^H(j2\omega) = H_2(j\omega,j\omega) = -\varepsilon_2\omega_L^2 H_1^2(j\omega)H_1(j2\omega), \tag{36}$$

$$G_3^H(j\omega) = H_3(-j\omega,j\omega,j\omega) = \omega_L^2\left[\frac{2}{3}\varepsilon_2^2(\omega_L^2 H_1(j2\omega)+2) - \varepsilon_3\right]H_1^2(j\omega)|H_1(j\omega)|^2, \tag{37}$$

$$G_3^H(j3\omega) = H_3(j\omega,j\omega,j\omega) = \omega_L^2(2\omega_L^2\varepsilon_2^2 H_1(j2\omega) - \varepsilon_3)H_1^3(j\omega)H_1(j3\omega), \tag{38}$$

$$G_4^H(j2\omega) = H_4(-j\omega,j\omega,j\omega,j\omega) = -\omega_L^2 H_1(j2\omega)[\varepsilon_2 H_{42}(j2\omega) + \varepsilon_3 H_{43}(j2\omega) + \varepsilon_4 H_{44}(j2\omega)], \tag{39}$$

$$G_4^H(j4\omega) = H_4(j\omega,j\omega,j\omega,j\omega) = -\omega_L^2 H_1(j4\omega)[\varepsilon_2 H_{42}(j4\omega) + \varepsilon_3 H_{43}(j4\omega) + \varepsilon_4 H_{44}(j4\omega)], \tag{40}$$

where

$$H_{42}(j2\omega) = H_{42}(-j\omega,j\omega,j\omega,j\omega) = \omega_L^2\left\{\left[\varepsilon_2^2\omega_L^2 H_1(j2\omega) - \frac{1}{2}\varepsilon_3\right]H_1(j3\omega) + \left[\varepsilon_2^2(\omega_L^2 H_1(j2\omega)+2) - \frac{3}{2}\varepsilon_3\right]H_1(j\omega) + \varepsilon_2^2 H_1(j2\omega)\right\}|H_1(j\omega)|^2 H_1^2(j\omega), \tag{41}$$

$$H_{43}(j2\omega) = H_{43}(-j\omega,j\omega,j\omega,j\omega) = -\frac{3}{2}\varepsilon_2[\omega_L^2 H_1(j2\omega)+1]H_1^2(j\omega)|H_1(j\omega)|^2, \tag{42}$$

$$H_{44}(j2\omega) = H_{44}(-j\omega,j\omega,j\omega,j\omega) = H_1^2(j\omega)|H_1(j\omega)|^2, \tag{43}$$

$$H_{42}(j4\omega) = H_{42}(j\omega,j\omega,j\omega,j\omega) = \omega_L^2\{[4\varepsilon_2^2\omega_L^2 H_1(j2\omega) - 2\varepsilon_3]H_1(j3\omega) + \varepsilon_2^2\omega_L^2 H_1^2(j2\omega)\}H_1^4(j\omega), \tag{44}$$

$$H_{43}(j4\omega) = -3\varepsilon_2\omega_L^2 H_1^4(j\omega)H_1(j2\omega), \tag{45}$$

$$H_{44}(j4\omega) = H_{44}(j\omega,j\omega,j\omega,j\omega) = H_1^4(j\omega). \tag{46}$$

4. Analysis of the resonance phenomena of the polynomial-type nonlinear systems

Resonance is a well-known phenomenon in engineering, which is an operating condition where an excitation frequency is near a natural frequency of machines or structures. When a resonance occurs for a

structure, the resulting vibration levels can be very high and this can cause considerable damage. In a machine that produces a broad vibration spectrum, a resonance shows up in the vibration spectrum as a peak. Depending on the effect of damping, the peak may be quite sharp or broad. As the dynamic properties of sodf linear systems can simply be described by the FRF, it is easy to investigate the resonance for linear systems. However, the resonance analysis of nonlinear systems is much more difficult. The concept of NOFRFs allows the analysis of a wide class of nonlinear systems to be implemented in a manner similar to the analysis of linear system frequency responses. Consequentially, the NOFRF concept provides a novel approach to the analysis of resonant phenomena of nonlinear systems.

4.1. The resonances and resonant frequencies of the NOFRFs

Consider the polynomial-type nonlinear system (2) subjected to a harmonic input (16). The output spectrum $Y(j\omega)$ of the system can be represented using the concept of NOFRFs as (25); and the contribution of the nth-order system nonlinearity to the system output spectrum is given by

$$Y_n(j\omega) = G_n^H(j\omega)A_n(j\omega), \quad n = 1, \ldots, N. \tag{47}$$

It is known from Eqs. (21) and (41) that in this case

$$Y_n(j\omega) = \begin{cases} Y_n(j(-n+2k)\omega_F) & = G_n^H(j(-n+2k)\omega_F)A_n(j(-n+2k)\omega_F) \\ & \text{when } \omega = (-n+2k)\omega_F, \quad k = 0, 1, \ldots, n, \\ 0 & \text{otherwise,} \end{cases} \tag{48}$$

Therefore, the magnitude of the NOFRF $G_n^H(j\omega)$ at frequency $\omega = (-n+2k)\omega_F$, $k = 0, 1, \ldots, n$ has a considerable effect on the nth-order system output spectrum. Consequently, the resonances and resonant frequencies of the NOFRF $G_n^H(j\omega)$ will be introduced and defined as follows.

Definition. For the polynomial-type nonlinear system (2) subjected to harmonic input (16), the resonant frequencies of the system nth-order NOFRF $G_n^H(j\omega)$ are those ω_F's which make any of $|G_n^H(j(-n+2k)\omega_F)|$, $k = 0, 1, \ldots, n$ reach a maximum, and the maxima reached will be referred to as the resonances.

For $n = 1$, $|G_n^H(j(-n+2k)\omega_F)|$, $k = 0, 1, \ldots, n$, are $|G_1^H(-j\omega_F)|$ and $|G_1^H(j\omega_F)|$. In order to determine the resonant frequencies, only the ω_F's which make $|G_1^H(j\omega_F)|$ reach a maximum need to be considered. Because

$$|G_1^H(j\omega_F)| = |H_1(j\omega_F)|. \tag{49}$$

It can be known that the resonant frequency of $G_1^H(j\omega_F)$ is $\omega_F = \omega_L$, and the corresponding resonance is $|G_1^H(j\omega_L)| = |H_1(j\omega_L)|$.

For $n = 2$, $|G_n^H(j(-n+2k)\omega_F)|$, $k = 0, 1, \ldots, n$, are $|G_2^H(-j2\omega_F)||G_2^H(0)|$ and $|G_2^H(j2\omega_F)|$. Therefore, the resonant frequencies of $|G_2^H(j\omega)|$ are the ω_F's which make $|G_2^H(j2\omega_F)|$ reach a maximum.

From Eq. (36)

$$|G_2^H(j2\omega_F)| = |H_2(j\omega_F, j\omega_F)| = \varepsilon_2\omega_L^2|H_1(j\omega_F)|^2|H_1(j2\omega_F)|. \tag{50}$$

Because $|H_1(j\omega_F)|$ reaches a maximum when $\omega = \omega_L$, Eq. (50) implies that the resonant frequencies of $G_2^H(j\omega)$ are $\omega_F = \omega_L$ and $\omega_F = \omega_L/2$, and the corresponding resonances are $\varepsilon_2\omega_L^2|H_1(j\omega_L)|^2|H_1(j2\omega_L)|$ and $\varepsilon_2\omega_L^2|H_1(j\omega_L/2)|^2|H_1(j\omega_L)|$.

For $n = 3$, $|G_n^H(j(-n+2k)\omega_F)|$, $k = 0, 1, \ldots, n$ are $|G_3^H(-j3\omega_F)|$, $|G_3^H(-j\omega_F)|$, $|G_3^H(j\omega_F)|$ and $|G_3^H(j3\omega_F)|$. Clearly, the resonant frequencies of $G_3^H(j\omega)$ are the ω_F's which make $|G_3^H(j\omega_F)|$ and $|G_3^H(j3\omega_F)|$ reach a maximum.

From Eqs. (37) and (38)

$$|G_3^H(j\omega_F)| = |H_3(-j\omega_F, j\omega_F, j\omega_F)| = \omega_L^2\left[\frac{2}{3}\varepsilon_2^2(\omega_L^2 H_1(j2\omega_F) + 2) - \varepsilon_3\right]|H_1(j\omega_F)|^4, \tag{51}$$

$$|G_3^H(j3\omega_F)| = |H_3(j\omega_F, j\omega_F, j\omega_F)| = \omega_L^2|2\omega_L^2\varepsilon_2^2 H_1(j2\omega_F) - \varepsilon_3||H_1(j\omega_F)|^3|H_1(j3\omega_F)|. \tag{52}$$

These results indicate that the resonant frequencies of $G_3^H(j\omega)$ are $\omega_F = \omega_L$ and $\omega_F = \omega_L/3$, and may also include $\omega_F = \omega_L/2$, and the corresponding resonances are $|H_3(-j\omega_L, j\omega_L, j\omega_L)|$, $|H_3(j\omega_L, j\omega_L, j\omega_L)|$; $|H_3(j\omega_L/3, j\omega_L/3, j\omega_L/3)|$; and $|H_3(-j\omega_L/2, j\omega_L/2, j\omega_L/2)|$, $|H_3(j\omega_L/2, j\omega_L/2, j\omega_L/2)|$.

For $n = 4$, $|G_n^H(j(-n+2k)\omega_F)|$, $k = 0, 1, \ldots, n$, are $|G_4^H(-j4\omega_F)|$, $|G_4^H(-j2\omega_F)|$, $|G_4^H(0)|$, $|G_4^H(j2\omega_F)|$ and $|G_4^H(j4\omega_F)|$. The resonant frequencies of $G_4^H(j\omega)$ are the ω_F's which make $|G_4^H(j2\omega_F)|$ and $|G_4^H(j4\omega_F)|$ reach a maximum.

Eqs. (39), (41)–(43) and (40), (44)–(46) show that

$$|G_4^H(j2\omega_F)| = |H_4(-j\omega_F, j\omega_F, j\omega_F, j\omega_F)| = \omega_L^2 |H_1(j2\omega_F)||H_1(j\omega_F)|^4 \times \left| \varepsilon_2 \omega_L^2 \left[\left(\varepsilon_2^2 \omega_L^2 H_1(j2\omega_F) - \frac{1}{2}\varepsilon_3 \right) H_1(j3\omega_F) + \left(\varepsilon_2^2 \omega_L^2 H_1(j2\omega_F) + 2\varepsilon_2^2 - \frac{3}{2}\varepsilon_3 \right) H_1(j\omega_F) + \varepsilon_2^2 H_1(j2\omega_F) \right] + \varepsilon_3 \left[-\frac{3}{2}\varepsilon_2 \left(\omega_L^2 H_1(j2\omega_F) + 1 \right) \right] + \varepsilon_4 \right| \tag{53}$$

and

$$|G_4^H(j4\omega_F)| = |H_4(j\omega_F, j\omega_F, j\omega_F, j\omega_F)| = \omega_L^2 |H_1(j4\omega_F)||H_1(j\omega_F)|^4 \quad |\varepsilon_2 \omega_L^2 [(4\varepsilon_2^2 \omega_L^2 H_1(j2\omega_F) - 2\varepsilon_3) H_1(j3\omega_F) + \varepsilon_2^2 \omega_L^2 H_1(j2\omega_F)] - 3\varepsilon_2 \varepsilon_3 \omega_L^2 H_1(j2\omega_F) + \varepsilon_4|. \tag{54}$$

Eqs. (53) and (54) imply that the resonant frequencies of $G_4^H(j\omega)$ are $\omega_F = \omega_L/4$, $\omega_F = \omega_L/2$ and $\omega_F = \omega_L$, and may also have $\omega_F = \omega_L/3$, and the corresponding resonances are $|H_4(j\omega_L/4, j\omega_L/4, j\omega_L/4, j\omega_L/4)|$; $|H_4(j\omega_L/2, j\omega_L/2, j\omega_L/2, j\omega_L/2)|$, $|H_4(-j\omega_L/2, j\omega_L/2, j\omega_L/2, j\omega_L/2)|$; $|H_4(j\omega_L, j\omega_L, j\omega_L, j\omega_L)|$, $|H_4(-j\omega_L, j\omega_L, j\omega_L, j\omega_L)|$; and $|H_4(j\omega_L/3, j\omega_L/3, j\omega_L/3, j\omega_L/3)|$, $|H_4(-j\omega_L/3, j\omega_L/3, j\omega_L/3, j\omega_L/3)|$.

Fig. 5 gives the NOFRFs of a nonlinear system with a 4th-order polynomial-type stiffness. The system parameters are $\varsigma = 0.12$, $\omega_L = 100\,\text{rad/s}$, $\varepsilon_2 = 300$, $\varepsilon_3 = 5 \times 10^4$, $\varepsilon_4 = 9 \times 10^5$. Clearly, the above general analysis is confirmed by this specific example.

4.2. Physical implication of the resonant frequencies of NOFRFs

In the study of the resonance of linear mechanical systems, it is known that when the driving frequency of the force matches the natural frequency of a vibrating system, the energy transmission is efficient, and the amplitude of the vibration becomes significant. Similarly, for nonlinear system which can be described by the polynomial-type nonlinear model (28), when the system subjected to a harmonic input and the driving frequency ω_F coincides with one of the resonant frequencies of an NOFRF of the system, the magnitude of this NOFRF will reach a maximum (resonance) at a high-order harmonic of ω_F. Consequently, considerable input signal energy may be transferred by the system from the driving frequency to the higher-order harmonic component. For example, when system (28) is subjected to a harmonic excitation with driving frequency $\omega_F = \omega_L/2$, which happens to be the resonant frequency of $G_3^H(j\omega)$ and $G_2^H(j\omega)$, a considerable input energy may be transferred through the 2nd-order NOFRF and the 3rd-order NOFRF from the driving frequency $\omega_L/2$ to the 2nd-order harmonic component $2(\omega_L/2) = \omega_L$ and the 3rd-order harmonic component $3\omega_L/2$ in the output. To demonstrate this, two harmonic inputs at the frequencies of $\omega_F = (3/2)\omega_L$ and $\omega_F = \omega_L/2$ were used respectively to excite system (28) with $\varsigma = 0.10$, and the other system parameters are the same as those used in Section 4.1. As Eqs. (25) and (27) indicate, if $N = 4$, then the 2nd-, 3rd- and 4th-order harmonics could appear in the system output frequency response, and the output spectrum can analytically be described as

$$Y(j\omega_F) = G_1^H(j\omega_F) A_1(j\omega_F) + G_3^H(j\omega_F) A_3(j\omega_F), \tag{55}$$

$$Y(j2\omega_F) = G_2^H(j2\omega_F) A_2(j2\omega_F) + G_4^H(j2\omega_F) A_4(j2\omega_F), \tag{56}$$

$$Y(j3\omega_F) = G_3^H(j3\omega_F) A_3(j3\omega_F), \tag{57}$$

$$Y(j4\omega_F) = G_4^H(j4\omega_F) A_4(j4\omega_F). \tag{58}$$

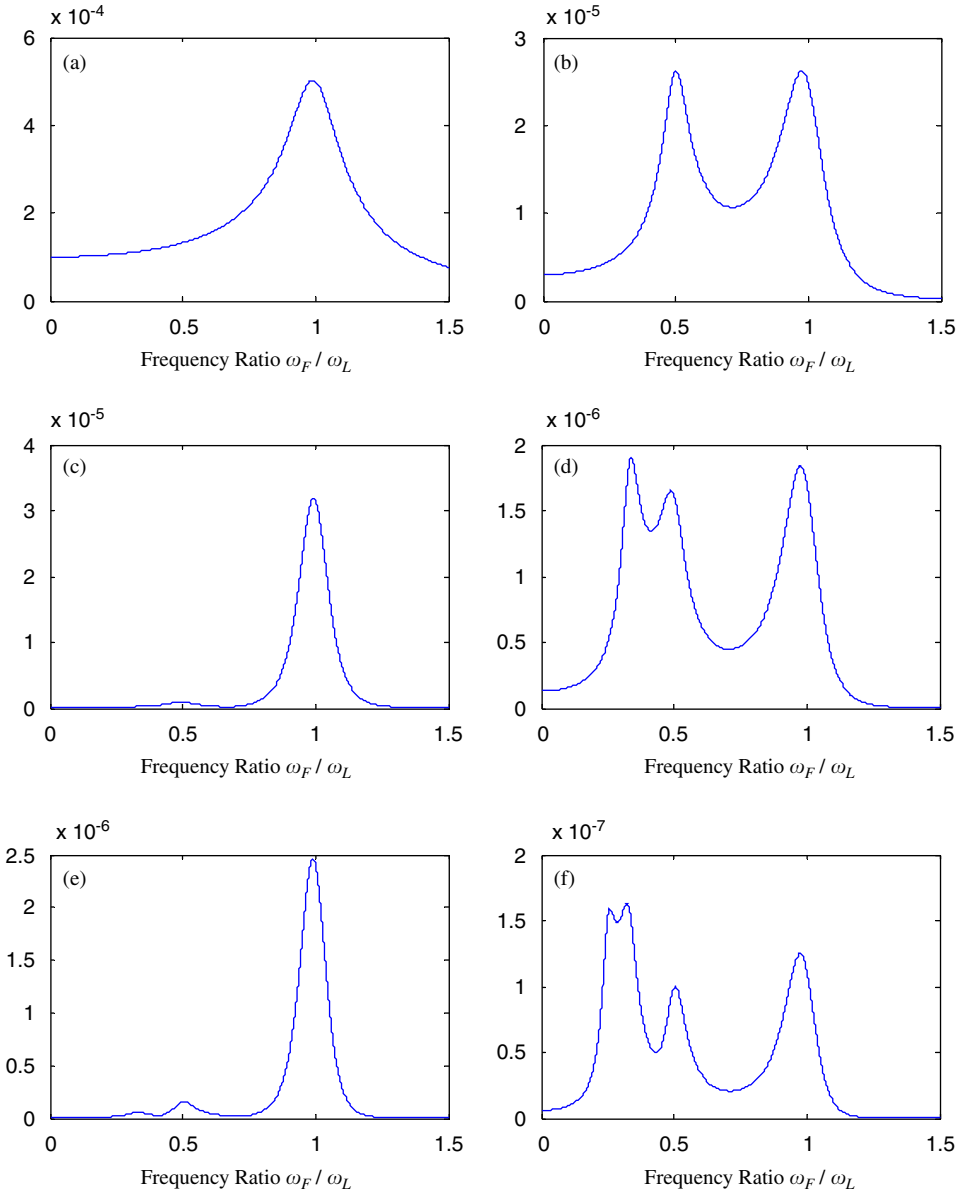

Fig. 5. The NOFRFs of a nonlinear system with a 4th-order polynomial-type stiffness under a harmonic loading: (a) $|G_1^H(j\omega_F)|$, (b) $|G_2^H(j2\omega_F)|$, (c) $|G_3^H(j\omega_F)|$, (d) $|G_3^H(j3\omega_F)|$, (e) $|G_4^H(j2\omega_F)|$, (f) $|G_4^H(j4\omega_F)|$.

As frequency $\omega_L/2$ is the resonant frequency of $G_2^H(j\omega)$ and $G_3^H(j\omega)$, which could make $|G_2^H(j\omega)|_{\omega=2(\omega_L/2)}$ and $|G_3^H(j\omega)|_{\omega=3(\omega_L/2)}$ reach a maximum, according to Eqs. (56) and (57), it is known that the 2nd- and 3rd-harmonic components of the output spectrum could be considerable when $\omega_F = \omega_L/2$. In contrast, when $\omega_F = 3\omega_L/2$ which is not the resonant frequencies of any of the NOFRFs involved in Eqs. (55)–(58), a significant high-order harmonic response should not be expected in the system output. Fig. 6 shows the spectra of the forced responses in the two cases of $\omega_F = \omega_L/2$ and $\omega_F = 3\omega_L/2$, which were obtained by integrating Eq. (28) using a fourth-order Runge–Kutta method. It can be seen from Fig. 6 that the 2nd- and 3rd-harmonic components in the case of $\omega_F = \omega_L/2$ are considerably more significant than in the case of $\omega_F = 3/2\omega_L$.

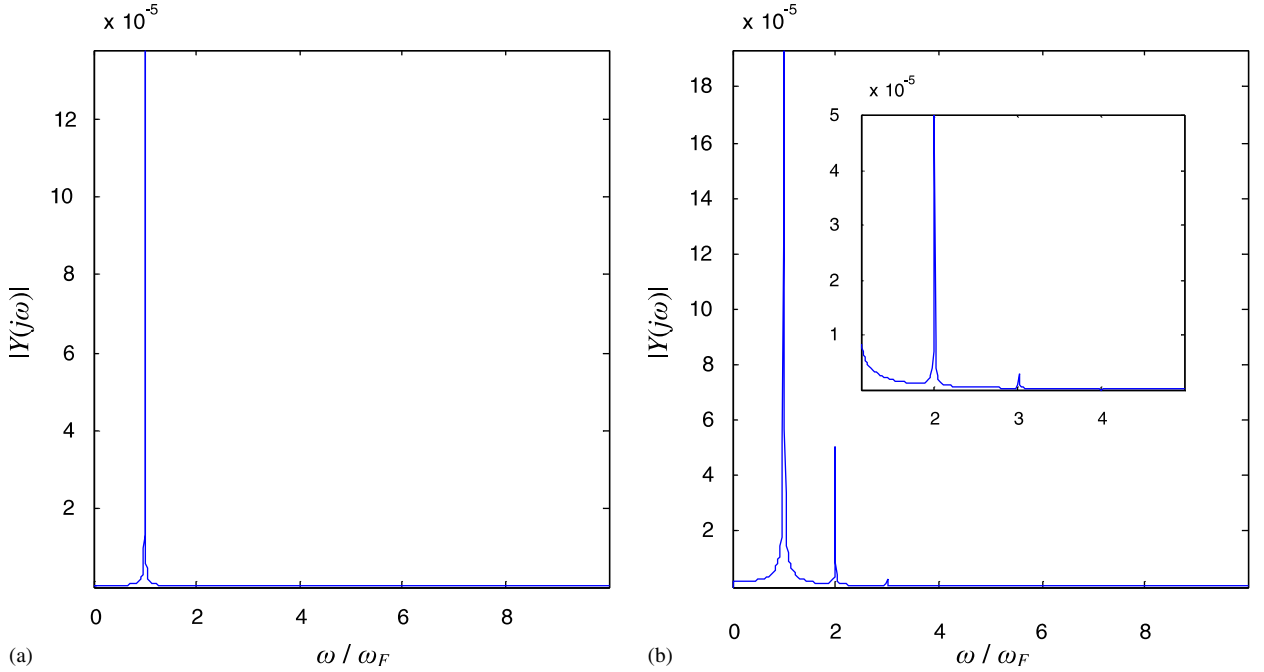

Fig. 6. An illustration of the physical implication of the resonant frequencies of NOFRFs: (a) $\omega = 1.5\omega_L$ (a non-resonant frequency of the involved NOFRFs) and (b) $\omega = 0.5\omega_L$ (a resonant frequency of the involved NOFRFs).

These observations lead to a novel interpretation regarding when significant energy transfer phenomena may take place with nonlinear systems subjected to a harmonic input. The interpretation is based on the concept of resonant frequencies of NOFRFs, and concludes that significant energy transfer phenomena may occur with a nonlinear system when the driving frequency of the harmonic input happens to be one of the resonances of the NOFRFs.

5. The effects of damping on the nonlinear resonant phenomena and output frequency responses

5.1. The effects of damping on the resonances

Damping refers to the dissipation of vibrational energy. All physical systems have some inherent damping. The effects of damping and stiffness [35] on linear structures are well understood. Basically speaking, damping is one of crucial factors that determine system behaviors. It is well known that the FRF $H_1(j\omega)$ of a damped linear system, defined by Eq. (29), has only one resonance at the frequency ω_L, and the amplitude of $H_1(j\omega)$ at ω_L is highly dependent on the damping coefficient ς, as given by

$$|H_1(j\omega_L)| = \frac{1}{2\varsigma\omega_L^2}. \tag{59}$$

Eq. (51) indicates that ς can reduce the system response at a resonant frequency, as shown in Fig. 7.

In the nonlinear case, the effects of damping on the NOFRFs are much more complicated. As Section 4.1 indicates, a higher-order NOFRF may have more than one resonant frequency. What is important is which resonant frequency may produce the biggest amplitude thus the dominant resonance for the NOFRF at a corresponding output frequency, and how the resonance of NOFRFs depends on the damping coefficient ς. The NOFRFs involve more complicated mathematical expressions than a linear FRF $H_1(j\omega)$, and are therefore difficult to study analytically. In the following, the effect of damping on the second-order NOFRF $G_2^H(j\omega)$ will be studied analytically, and the other NOFRFs will be investigated using simulation studies.

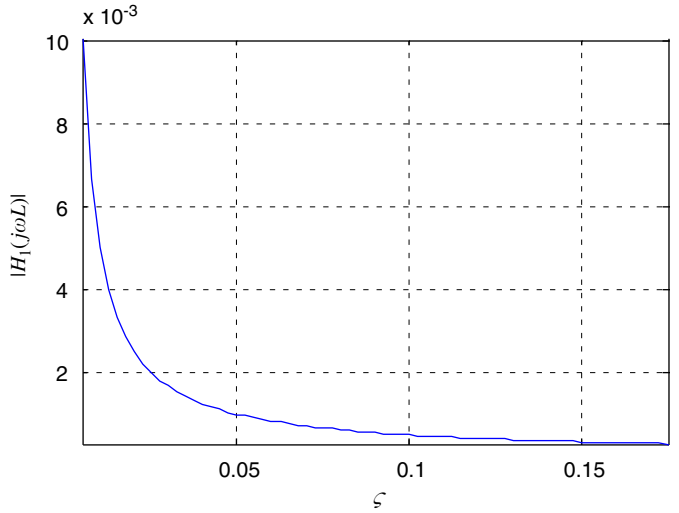

Fig. 7. The dependence of an FRF at the resonant frequency ω_L on the damping coefficient ς.

Define λ as the ratio between the amplitudes of the two resonances of $G_2^H(j\omega)$, $|G_2^H(j2\omega_F)|_{\omega_F=\omega_L/2}$ and $|G_2^H(j2\omega_F)|_{\omega_F=\omega_L}$, so that

$$\lambda = \frac{|G_2^H(j2\omega_L/2)|}{|G_2^H(j2\omega_L)|} = \frac{|H_1^2(j\omega_L/2)H_1(j2\omega_L/2)|}{|H_1^2(j\omega_L)H_1(j2\omega_L)|} = \frac{|H_1^2(j\omega_L/2)|}{|H_1(j\omega_L)H_1(j2\omega_L)|}. \tag{60}$$

Substituting (29) into (60) yields

$$\begin{aligned}\lambda &= \frac{|H_1^2(j\omega_L/2)|}{|H_1(j\omega_L)H_1(j2\omega_L)|} = \frac{|j2\varsigma\omega_L^2(-3\omega_L^2 + j4\varsigma\omega_L^2)|}{\left|\left(\frac{3}{4}\omega_L^2 + j\varsigma\omega_L^2\right)\left(\frac{3}{4}\omega_L^2 + j\varsigma\omega_L^2\right)\right|} \\ &= \frac{|j2\varsigma(-3 + j4\varsigma)|}{\left|\left(\frac{3}{4} + j\varsigma\right)\left(\frac{3}{4} + j\varsigma\right)\right|}.\end{aligned} \tag{61}$$

That is

$$\lambda = \frac{32\varsigma}{\sqrt{9 + 16\varsigma^2}} = \frac{32}{\sqrt{9/\varsigma^2 + 16}}. \tag{62}$$

Eq. (62) shows that λ only depends on the damping coefficient ς, and λ will increase with increasing ς. When $\varsigma = \sqrt{9/(32^2 - 16)} \approx 0.0945$, λ is equal to 1.0, that is, the two resonances of $G_2^H(j\omega)$ have the same amplitudes. When ς is smaller than 0.0945, the resonance at ω_L will be larger than the resonance at $\omega_L/2$, so that the resonance at ω_L becomes the dominant resonance. On the contrary, when ς is larger than 0.0945, the resonance at $\omega_L/2$ becomes the dominant resonance. Fig. 8 shows this dependence of λ on the damping coefficient ς.

In addition, from Eq. (36), it is known that the amplitude of the resonance of $G_2^H(j\omega)$ at $\omega_L/2$ can be written as

$$|G_2^H(j2\omega_L/2)| = \varepsilon_2\omega_L^2|H_1^2(j\omega_L/2)H_1(j\omega_L)| = \frac{8\varepsilon_2}{\omega_L^4}\frac{1}{\varsigma(9 + 16\varsigma^2)}. \tag{63}$$

Eq. (63) indicates that $|G_2^H(j2\omega_L/2)|$ decreases sharply with ς over the range $0.005 \leqslant \varsigma \leqslant 0.17$ when $\omega_L = 100$ rad/s. Fig. 9 shows this analytical relationship.

To investigate the effects of the damping coefficient on other NOFRFs, numerical methods were used. The fourth-order polynomial-type nonlinear system used in Section 4.1 was used for the simulation study with the damping coefficient ς changing between 0.005 and 0.175. The external force $f_0(t)$ considered was a sinusoidal force with unit amplitude and frequency ω_F which was varied within the range of $0 \leqslant \omega_F \leqslant 1.5\omega_L$.

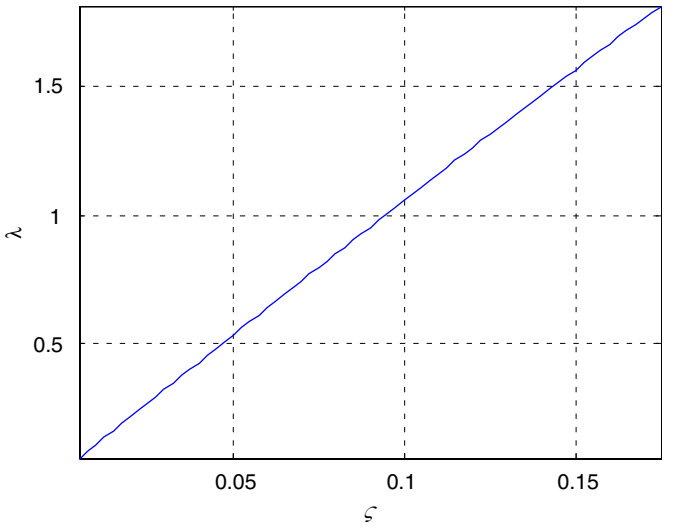

Fig. 8. The dependence of λ on damping coefficient ς.

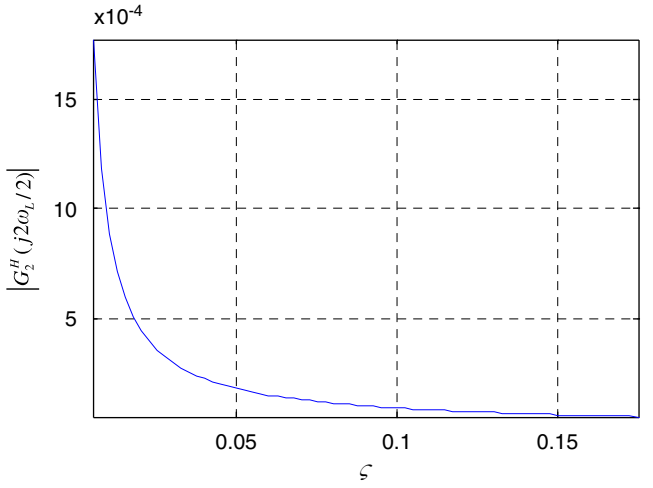

Fig. 9. The dependence of $|G_2^H(j2\omega_L/2)|$ on damping coefficient ς when $\omega_L = 100$ rad/s.

The NOFRFs up to 4th-order were analyzed. Figs. 10–14 give the results of, $|G_2^H(j2\omega_F)|$, $|G_3^H(j\omega_F)|$, $|G_3^H(j3\omega_F)|$, $|G_4^H(j2\omega_F)|$ and $|G_4^H(j4\omega_F)|$ respectively. In order to avoid the situation where the NOFRFs with a considerable amplitude overdominate the plots and make NOFRFs with a relatively small amplitude hardly observable, the normalized NOFRFs were used in Figs. 10–14, which were defined by

$$\overline{\mathrm{NOFRF}}(j\omega_F) = \frac{\mathrm{NOFRF}(j\omega_F)}{\max_{0\leqslant\omega_F\leqslant 1.5\omega_L}(|\mathrm{NOFRF}(j\omega_F)|)}. \tag{64}$$

Fig. 10 clearly shows that $|G_2^H(j2\omega_F)|$reaches two maxima at $\omega_F = \omega_L$ and $\omega_F = \omega_L/2$, the two resonant frequencies of $G_2^H(j\omega)$. When the damping coefficient ς is small, the maximum at $\omega_F = \omega_L$ is larger than the resonance at $\omega_F = \omega_L/2$. As ς increases, the resonance at $\omega_F = \omega_L/2$ becomes more and more significant, and around $\varsigma = 0.09$, the maximum at $\omega_F = \omega_L/2$ overwhelms the one at ω_L and becomes the dominant resonance of $|G_2^H(j\omega)|$. These results confirm the analytical analysis results about the resonances of $|G_2^H(j\omega)|$. From Eq. (37), it is known that $|G_3^H(j\omega_F)|$ may have two maxima at $\omega_F = \omega_L$ and $\omega_F = \omega_L/2$, the appearance of the two maxima in Fig. 11 confirms this. It can be found that the maximum at $\omega_F = \omega_L/2$ is very small and hardly

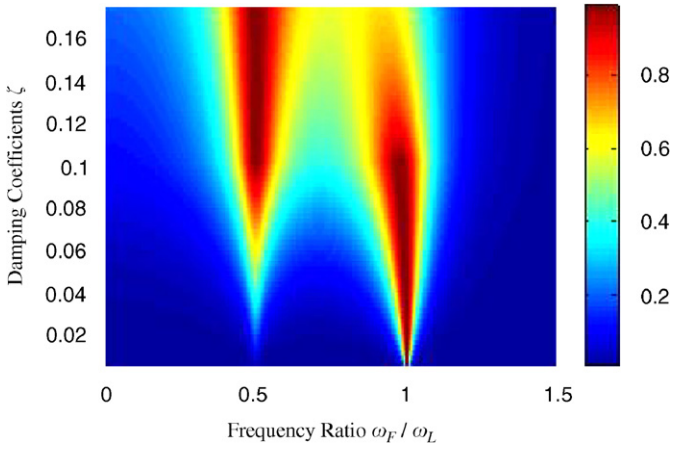

Fig. 10. $\left|\overline{G_2^H(j2\omega_F)}\right|$ at different damping coefficients.

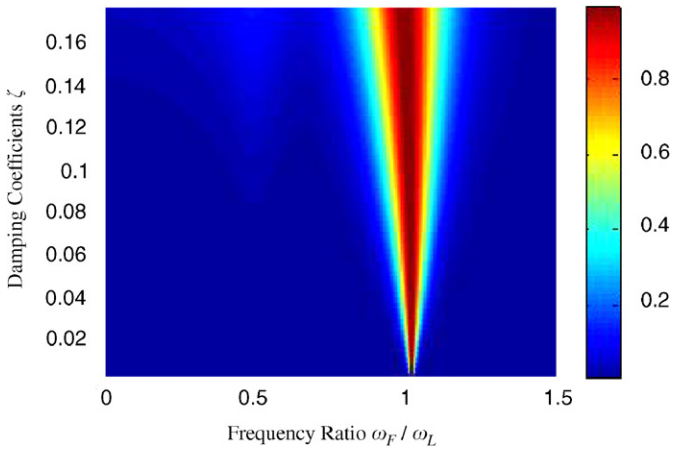

Fig. 11. $\left|\overline{G_3^H(j\omega_F)}\right|$ at different damping coefficients.

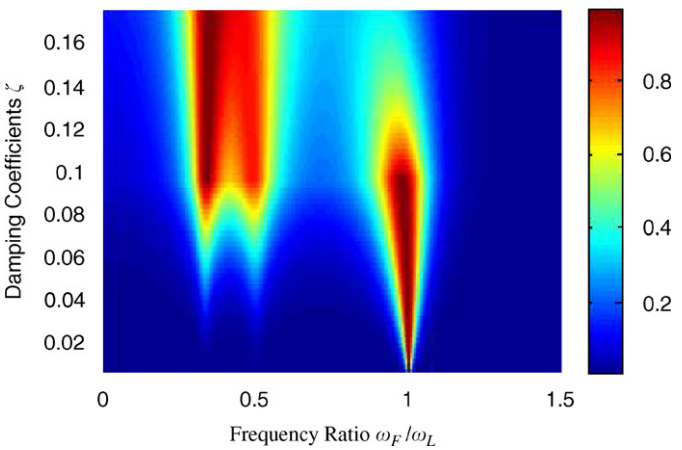

Fig. 12. $\left|\overline{G_3^H(j3\omega_F)}\right|$ at different damping coefficients.

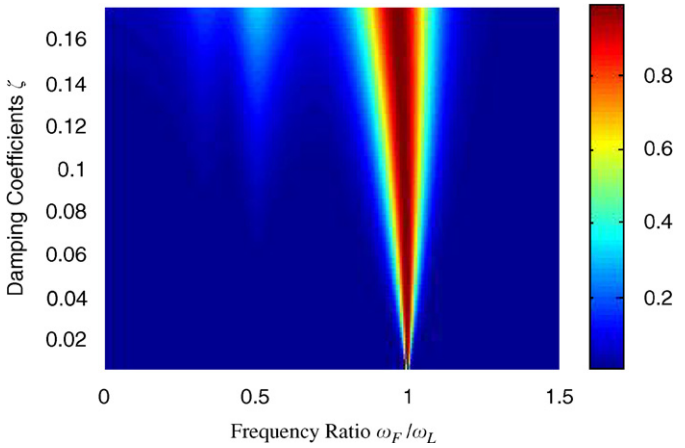

Fig. 13. $\left|\overline{G_4^H(j2\omega_F)}\right|$ at different damping coefficients.

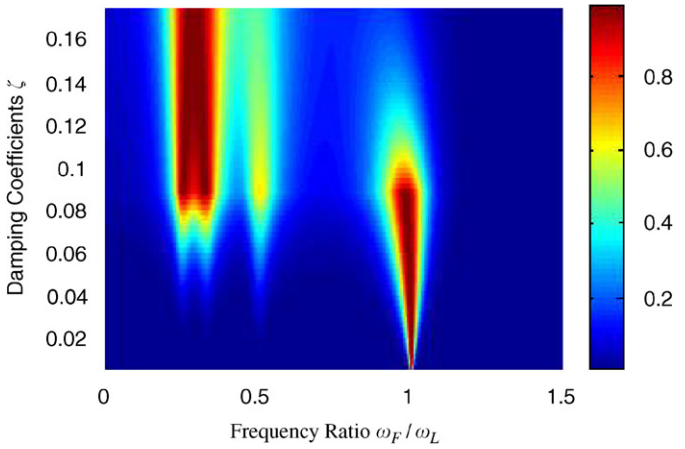

Fig. 14. $\left|\overline{G_4^H(j4\omega_F)}\right|$ at different damping coefficients.

observable, especially over the region of $\varsigma<0.1$. Therefore, for $G_3^H(j\omega)$, the resonance at $\omega_F=\omega_L$ is always the dominant resonance compared with the resonance at $\omega_F=\omega_L/2$. Eq. (38) shows that $|G_3^H(j3\omega_F)|$ may produce three maxima at $\omega_F=\omega_L$, $\omega_F=\omega_L/2$ and $\omega_F=\omega_L/3$, all of which are shown clearly in Fig. 12. According to Fig. 12, when $\varsigma<0.09$, the maximum at $\omega_F=\omega_L$ is larger than the two others, and therefore is the dominant resonance, but when $\varsigma>0.09$, the maximum at $\omega_F=\omega_L/3$ becomes dominant. Eqs. (39), (41)–(43) indicate that $|G_4^H(j2\omega_F)|$ has three possible maxima at $\omega_F=\omega_L$, $\omega_F=\omega_L/2$ and $\omega_F=\omega_L/3$. Fig. 13 confirms this, and indicates that the maximum at $\omega_F=\omega_L$ is always dominant, while the other two are very weak and observable only in the region of $\varsigma>0.09$. Fig. 14 clearly shows that $|G_4^H(j4\omega_F)|$ has four maxima at $\omega_F=\omega_L$, $\omega_F=\omega_L/2$, $\omega_F=\omega_L/3$ and $\omega_F=\omega_L/4$. Just like the other NOFRFs, when ς is small, the maximum at $\omega_F=\omega_L$ is the dominant resonance and larger than the others, and when ς is increased, the dominant resonance swifts to the other resonant frequencies. In the case shown in Fig. 14, the resonances at $\omega_F=\omega_L/3$ and $\omega_F=\omega_L/4$ have nearly the same amplitudes.

5.2. The effect of damping on the output frequency responses

The analysis above shows that, since both $\omega_F=\omega_L$ and $\omega_F=\omega_L/2$ are the resonant frequencies of $G_2^H(j\omega)$ and $G_4^H(j\omega)$, and each could make $|G_2^H(j2\omega_F)|$ and $|G_4^H(j2\omega_F)|$ reach a maximum. It follows therefore that the second harmonic component $Y(j2\omega_F)$ will achieve a significant amplitude when $\omega_F=\omega_L$ and $\omega_F=\omega_L/2$.

Moreover, it is also known from the above analysis that if the damping coefficient ς is smaller than 0.0945, $|Y(j2\omega_F)|$ at $\omega_F = \omega_L$ will be larger than that at $\omega_F = \omega_L/2$ because, under this condition, the resonance at $\omega_F = \omega_L$ is the dominant resonance for both $G_2^H(j\omega)$ and $G_4^H(j\omega)$. On the contrary, if $\varsigma > 0.0945$, then $|Y(j2\omega_F)|$ at $\omega_F = \omega_L/2$ will be larger than the resonance at $\omega_F = \omega_L$. In this case, the dominant resonance of $G_2^H(j\omega)$ shifts from $\omega_F = \omega_L$ to $\omega_F = \omega_L/2$, $|Y(j2\omega_F)|$ is mainly determined by $G_2^H(j2\omega_F)A_2(j2\omega_F)$, and the contribution of $G_4^H(j2\omega_F)A_4(j2\omega_F)$ to $|Y(j2\omega_F)|$ is less significant.

In order to justify these analysis results, harmonic inputs at the frequencies of $\omega_F = \omega_L$ and $\omega_F = 1/2\omega_L$ were used, respectively, to excite the model used in Section 4.1 with $\varsigma = 0.06$ and 0.15, respectively. The output spectra are shown in Figs. 15–18. The forced system responses were obtained by integrating Eq. (28) using a

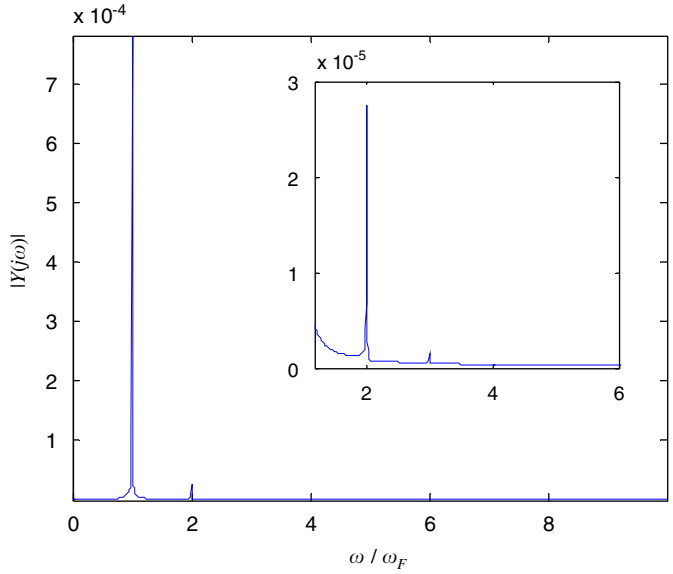

Fig. 15. Output spectrum ($\varsigma = 0.06$, and $\omega_F = \omega_L$).

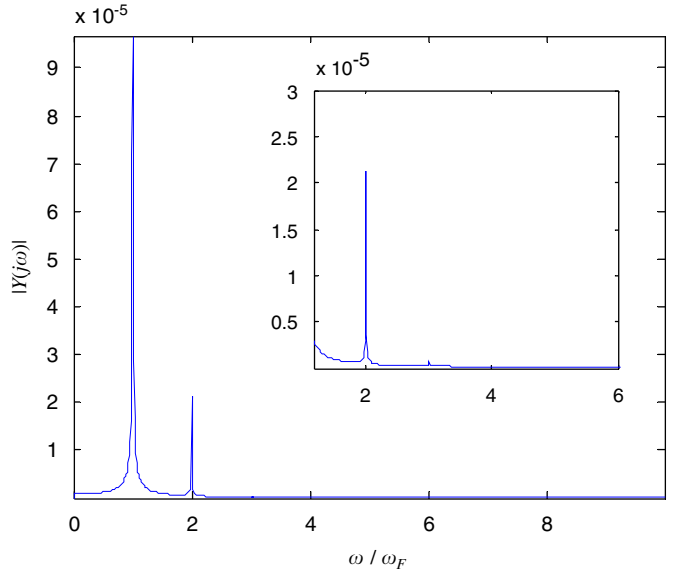

Fig. 16. Output spectrum ($\varsigma = 0.06$, and $\omega_F = 1/2\omega_L$).

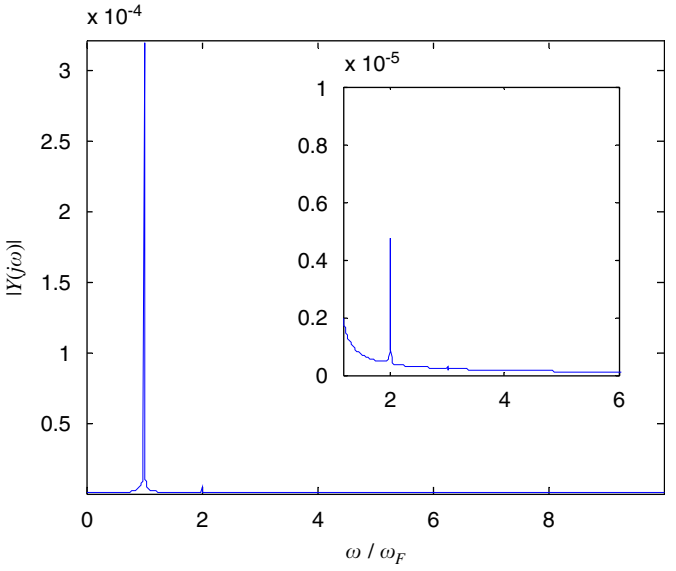

Fig. 17. Output spectrum ($\varsigma = 0.15$, and $\omega_F = \omega_L$).

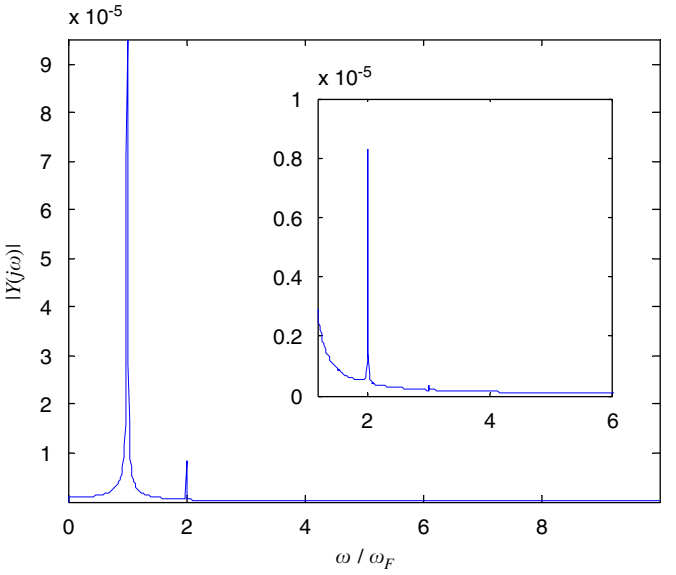

Fig. 18. Output spectrum ($\varsigma = 0.15$, and $\omega = \omega_L/2$).

fourth-order Runge–Kutta method. It can be seen from Figs. 15–18 that, for all ς, the first harmonics at $\omega_F = \omega_L$ are always larger than those at $\omega_F = \omega_L/2$, This arises because ω_L is the only resonant frequency of $G_1^H(j\omega)$. Whereas, in the case of $\varsigma = 0.06$, the second harmonic at $\omega_F = \omega_L$ is larger than that at $\omega_F = \omega_L/2$. However, in the case of $\varsigma = 0.15$, the second harmonic at $\omega_F = \omega_L$ is smaller than that at $\omega_F = \omega_L/2$. This result is completely consistent with the analytical study results about the effects of the damping coefficient on the second order NOFRF $G_2^H(j\omega)$, i.e., the damping coefficient determines the dominant resonance frequency of the NOFRF.

In mechanical engineering studies [36], the appearance of superharmonic components in the output spectrum is considered to be a significant nonlinear effect. From the perspective of the energy transfer, it is the linear FRF which transfers the input energy to the fundamental harmonic component in the output spectrum,

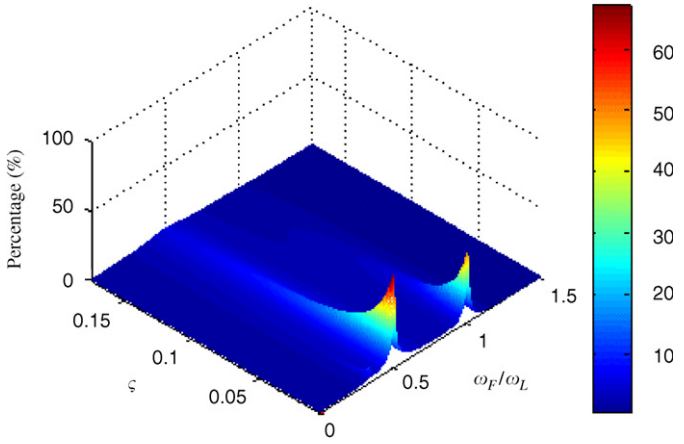

Fig. 19. The percentage of the whole energy that the superharmonic components contain at different driving frequencies and different damping coefficients.

and it is the NOFRFs which transfer the input energy to the superharmonic components. Therefore, to a certain extent, if the superharmonic components contain more energy in the output spectrum, then the nonlinear effects of a nonlinear system can be said to be stronger. Fig. 19 shows the percentage of the whole output energy that the superharmonic components contain at different driving frequencies ω_F for different damping coefficients ς. It can be seen that there are two strong peaks at the frequencies of $\omega_F = 1/2\omega_L$ and $\omega_F = \omega_L$ in the plot, which means the superharmonic components make a significant contribution to the total output energy when the driving frequency happens to be at $1/2\omega_F$ and ω_L. This implies that, when the class of nonlinear systems investigated in the present study work at about half the natural frequency, more energy will be transferred to the superharmonic frequency locations, and the nonlinear system will thus render a strong nonlinear response. Moreover, it can be found that, for all ς, the peaks at $\omega_F = 1/2\omega_L$ are always larger than those at $\omega_F = \omega_L$. This follows because, in the cases of smaller ς, $\omega_F = 1/2\omega_L$ is not the dominant resonant frequency for all NOFRFs and, consequently, the corresponding higher harmonic components will not be as strong as they are at $\omega_F = \omega_L$, and hence the first harmonic component will be significantly reduced when the driving frequency shifts from $\omega_F = \omega_L$ to $\omega_F = 1/2\omega_L$. This significant decrease in the first harmonic component causes the total output energy of the system to reduce, therefore the whole energy contained by the superharmonic components are on a relatively high level only for $\omega_F = 1/2\omega_L$. This implies that, the dominant nonlinear effects will be more apparent when the system is excited at half the resonant frequency. This observation is clearly of considerable significance for detection of faults in a system which make the system behave nonlinearly. In addition, from Fig. 19, it can be seen that, with the augment of ς, the energy contained in the superharmonic components will decrease sharply. This is because the reduction of the amplitude of the Nth-order NOFRF with ς approximately follows the law $(1/\varsigma^N)$, therefore the higher-order superharmonic components will decrease sharply with increasing ς. Comparatively, the decrease of the first harmonic component will be relatively slow. The sharp decrease of the higher-order superharmonic components with the augment of ς indicates that the nonlinear effects will not be apparent for a heavily damped nonlinear system.

In summary, the analysis in this section indicates that the damping effects affect the dominant resonant frequency of the NOFRFs. But whatever value the damping ratio ς is, the percentage that the superharmonic components take over the whole signal energy always reaches maximum when $\omega_F = 1/2\omega_L$. This is an important point for system fault detection. In addition, the analysis also implies that a heavily damped nonlinear system will act more linearly than a nonlinear system with weak damping properties.

6. Conclusions and remarks

The concept of resonances and resonant frequencies for sdof nonlinear systems with a polynomial-type stiffness, which can be used to model a wide range of practical vibration components with nonlinear stiffness

characteristics, has been introduced based on the NOFRFs. A detailed analysis of the effects of damping on the resonant phenomena of this class of nonlinear systems has also been conducted.

Many commonly used nonlinear models can be approximated by a polynomial-type nonlinear model, which can be analyzed using the Volterra series theory of nonlinear systems, and this forms the basis of the concept of NOFRFs. Based on the NOFRF concept, the definition of resonances and resonant frequencies of nonlinear systems has been introduced in this paper , and it has been revealed that all higher-order NOFRFs generally have more than one resonance which usually appears when the driving frequency is ω_L, $1/2\omega_L$, $1/3\omega_L$, $1/4\omega_L$, *etc* with ω_L being the natural frequency of the system. Furthermore, the analysis of the effects of damping on the resonances shows that, when the damping coefficient is small, the dominant resonant frequency of the high-order NOFRFs is the same as the resonant frequency ω_L of the first-order NOFRF. However, if the damping coefficient is large enough, the dominant resonance will shift to new frequencies, for example, to $1/2\omega_L$ for the second NOFRF. In addition, the amplitudes of the higher-order NOFRFs will decrease sharply with the argument of the damping coefficient. Generally, if the order of an NOFRF is higher, the amplitude will decrease sharply with the augment of ς. These are important conclusions relating to the resonant phenomenon of polynomial-type nonlinear systems, and are of practical significance for system design. For example, the design of a vibration control device for a nonlinear systems. Another important conclusion is that the polynomial-type nonlinear system always exhibits the strongest nonlinearity at the driving frequency of $\omega_F = 1/2\omega_L$, no matter how large the damping coefficient is. Since nonlinear effects are significant features for detecting cracks in structures, this conclusion is of importance for structural fault diagnosis. From this conclusion, one can know that, when using a sinusoidal excitation to carry out the crack detection procedure, the frequency of the excitation is better to be $1/2\omega_L$.

Acknowledgments

The authors gratefully acknowledge the support of the Engineering and Physical Science Research Council, UK, for this work.

References

[1] H.K. Jang, Design guideline for the improvement of dynamic comfort of a vehicle seat and its application, *International Journal of Automotive Technology* 6 (2005) 383–390.
[2] B.S. Yang, S.P. Choi, Y.C. Kim, Vibration reduction optimum design of a steam-turbine rotor-bearing system using a hybrid genetic algorithm, *Structural and Multidisciplinary Optimization* 30 (2005) 43–53.
[3] P. Museros, E. Alarcon, Influence of the second bending mode on the response of high-speed bridges at resonance, *Journal of Structural Engineering—ASCE* 131 (2005) 405–415.
[4] N. Jalili, D.W. Knowles, Structural vibration control using an active resonator absorber: modeling and control implementation, *Smart Materials and Structures* 13 (2004) 998–1005.
[5] A. Maccari, Vibration control for the primary resonance of a cantilever beam by a time delay state feedback, *Journal of Sound and Vibration* 259 (2003) 241–251.
[6] E.A. Butcher, Clearance effects on bilinear normal mode frequencies, *Journal of Sound and Vibration* 224 (1999) 305–328.
[7] P. Metallidis, S. Natsiavas, Vibration of a continuous system with clearance and motion constraints, *International Journal of Non-linear Mechanics* 35 (2000) 675–690.
[8] D. Pun, S.L. Lau, Y.B. Liu, Internal resonance of an L-shaped beam with a limit stop I, free vibration, *Journal of Sound and Vibration* 193 (1996) 1023–1035.
[9] D. Pun, S.L. Lau, Y.B. Liu, Internal resonance of an L-shaped beam with a limit stop II, forced vibration, *Journal of Sound and Vibration* 193 (1996) 1037–1047.
[10] A. Rivola, P.R. White, Bispectral analysis of the bilinear oscillator with application to the detection of fatigue cracks, *Journal of Sound and Vibration* 216 (1998) 889–910.
[11] M. Chati, R. Rand, S. Mukherjee, Modal analysis of a cracked beam, *Journal of Sound and Vibration* 207 (1997) 249–270.
[12] D. Goge, M. Sinapius, U. Fullekrug, M. Link, Detection and description of non-linear phenomena in experimental modal analysis via linearity plots, *International Journal of Non-linear Mechanics* 40 (2005) 27–48.
[13] R. Gasch, A survey of the dynamic behaviour of a simple rotating shaft with a transverse crack, *Journal of Sound and Vibration* 160 (1993) 313–332.
[14] N. Pugno, R. Ruotolo, C. Surace, Analysis of the harmonic vibrations of a beam with a breathing crack, *Proceedings of the 15th IMAC*, Tokyo, Japan, 1997, pp. 409–413.

[15] A.K. Darpe, K. Gupta, A. Chawla, Transient response and breathing behaviour of a cracked Jeffcott rotor, *Journal of Sound and Vibration* 272 (2004) 207–243.
[16] H. Yabuno, Y. Endo, N. Aoshima, Stabilization of 1/3-order subharmonic resonance using an autoparametric vibration absorber, *Journal of Vibration and Acoustics—Transactions of the ASME* 121 (1999) 309–315.
[17] N. Wiener, *Nonlinear Problems in Random Theory*, Wiley, New York, 1958.
[18] M. Schetzen, *The Volterra and Wiener Theories of Nonlinear Systems*, Krieger, Malabar, 1980.
[19] K. Worden, G. Manson, G.R. Tomlinson, A harmonic probing algorithm for the multi-input Volterra series, *Journal of Sound and Vibration* 201 (1997) 67–84.
[20] Z.Q. Lang, S.A. Billings, Output frequency characteristics of nonlinear system, *International Journal of Control* 64 (1996) 1049–1067.
[21] S.A. Billings, K.M. Tsang, Spectral analysis for nonlinear system, part I: parametric non-linear spectral analysis, *Mechanical Systems and Signal Processing* 3 (1989) 319–339.
[22] S.A. Billings, J.C. Peyton Jones, Mapping nonlinear integro-differential equations into the frequency domain, *International Journal of Control* 52 (1990) 863–879.
[23] J.C. Peyton Jones, S.A. Billings, A recursive algorithm for the computing the frequency response of a class of nonlinear difference equation models, *International Journal of Control* 50 (1989) 1925–1940.
[24] H. Zhang, S.A. Billings, Analysing non-linear systems in the frequency domain, I: the transfer function, *Mechanical Systems and Signal Processing* 7 (1993) 531–550.
[25] H. Zhang, S.A. Billings, Analysing nonlinear systems in the frequency domain, II: the phase response, *Mechanical Systems and Signal Processing* 8 (1994) 45–62.
[26] Z.Q. Lang, S.A. Billings, Energy transfer properties of nonlinear systems in the frequency domain, *International Journal of Control* 78 (2005) 354–362.
[27] J.S. Bae, D.J. Inman, I. Lee, Effects of structural nonlinearity on subsonic aeroelastic characteristics of an aircraft wing with control surface, *Journal of Fluids and Structures* 19 (2004) 747–763.
[28] T. Sun, H. Hu, Nonlinear dynamics of a planetary gear system with multiple clearances, *Mechanism and Machine Theory* 38 (2003) 1371–1390.
[29] H. Jeffreys, B.S. Jeffreys, *Methods of Mathematical Physics*, third ed., Cambridge University Press, Cambridge, England, 1988.
[30] S.A. Billings, Z.Q. Lang, Non-linear systems in the frequency domain: energy transfer filters, *International Journal of Control* 75 (2002) 1066–1081.
[31] G.M. Lee, Estimation of non-linear system parameters using higher-order frequency response functions, *Mechanical Systems and Signal Processing* 11 (1997) 219–229.
[32] J.A. Vazquez Feijoo, K. Worden, R. Stanway, Associated linear equations for Volterra operators, *Mechanical Systems and Signal Processing* 19 (2005) 57–69.
[33] J.A. Vazquez Feijoo, K. Worden, R. Stanway, System identification using associated linear equations, *Mechanical Systems and Signal Processing* 18 (2004) 431–455.
[34] J.A. Vazquez Feijoo, K. Worden, R. Stanway, Analysis of time-invariant systems in the time and frequency domain by associated linear equations (ALEs), *Mechanical Systems and Signal Processing* 20 (2006) 896–919.
[35] J. Woodhouse, Linear damping models for structural vibration, *Journal of Sound and Vibration* 215 (1998) 547–569.
[36] A.P. Bovsunovskya, C. Surace, Considerations regarding superharmonic vibrations of a cracked beam and the variation in damping caused by the presence of the crack, *Journal of Sound and Vibration* 288 (2005) 865–886.